applied sciences

MDPI

*Article*

# Fatigue Crack Calculation of Steel Structure Based on the Improved McEvily Model

**Zuocao Yu, Jiyi Wu *, Kaijiang Ma, Chenjie Zhong and Chunyun Jiang**

Institute of Bridge Engineering, Zhejiang University of Technology, Hangzhou 310023, China; wzyzc@zjut.edu.cn (Z.Y.); makaijiang@zjut.edu.cn (K.M.); zcj@zjut.edu.cn (C.Z.); jiangcy@zjut.edu.cn (C.J.)
* Correspondence: wu-jiyi@zjut.edu.cn

**Abstract:** Numerous fatigue crack mechanism models have been proposed based on an in-depth study of material fatigue mechanisms and engineering requirements. However, due to many of the parameters in these models being difficult to determine, their application to engineering is limited. The fatigue crack of the steel structure was calculated based on the improved McEvily model. To begin, based on the theory of linear elastic fracture mechanics, some parameters of the McEvily fatigue crack growth model were deduced and determined by using more reasonable assumptions and empirical formulas. Second, the effectiveness of the improved McEvily fatigue crack growth model was proven by comparison to the results of the improved model with the classical Paris model. Finally, the improved McEvily model was applied to practical engineering, and the typical fatigue crack of steel structure was selected and compared with the results of the Paris model and nominal stress method to verify its feasibility in engineering. The results reveal that the application conditions of the improved McEvily model can be extended from laboratory conditions to practical engineering, and its accuracy is better than that of the Paris model, which can well evaluate the fatigue crack life of steel structures.

**Keywords:** steel structure; fatigue crack growth model; improved McEvily model; Paris model; fatigue damage

check for updates

**Citation:** Yu, Z.; Wu, J.; Ma, K.; Zhong, C.; Jiang, C. Fatigue Crack Calculation of Steel Structure Based on the Improved McEvily Model. *Appl. Sci.* **2022**, *12*, 6344. https://doi.org/10.3390/app12136344

Academic Editor: Abílio M.P. De Jesus

Received: 16 May 2022
Accepted: 20 June 2022
Published: 22 June 2022

**Publisher's Note:** MDPI stays neutral with regard to jurisdictional claims in published maps and institutional affiliations.

**Copyright:** © 2022 by the authors. Licensee MDPI, Basel, Switzerland. This article is an open access article distributed under the terms and conditions of the Creative Commons Attribution (CC BY) license (https://creativecommons.org/licenses/by/4.0/).

## 1. Introduction

Nowadays, orthotropic steel decks have been widely used in modern bridge structures, with outstanding advantages such as high bearing capacity, light weight, and wide application range [1,2]. However, Orthotropic steel bridge decks are directly loaded by vehicle tires during the service period, easily resulting in the accumulation of fatigue damage and fatigue cracks, which have become an important factor affecting structural safety. Since the first report of fatigue cracks in the Orthotropic steel deck of Severn Bridge in 1971, numbers of fatigue cracking damages have been found in bridges worldwide of Orthotropic steel deck [3]. According to the investigation of Imam et al. [4], the proportion of fatigue damage in the failure of the bridge structure with or without collapse is 13% and 67%, respectively. Therefore, the fatigue life assessment of orthotropic plates is very important for bridge safety [5–7].

The fatigue crack growth rate curve is the basic material characteristic of steel structures under fatigue load, and a good fatigue crack growth model plays a vital role in fatigue life evaluation [8,9]. In order to accurately simulate the criterion of fatigue crack growth, some fatigue crack growth models have been proposed. The first crack growth rate based on linear elastic fracture mechanics was introduced by Paris [10], who equated fatigue crack growth rate by using amplitude stress intensity factor. Forman et al. [11] improved on the basis of the Paris model and modified the exponential crack growth model to cover the effects owing to the load ratio and the maximum stress-intensity factor. McEvily et al. [12] proposed a modified constitutive model introducing the concept of

crack closure and effective stress intensity factor $K_{eff}$. While the Paris model is the most extensively utilized at the moment, it has several limitations: First, the Paris model with the same material constant cannot explain the effect of crack growth under different load ratios ($R = K_{min}/K_{max}$). Second, the Paris model cannot include the entire process of crack growth. Due to the aforementioned limitations, the reliability of the Paris model results in the structural fatigue life prediction in practical engineering remains to be discussed to confirm. As one of the fatigue crack growth models, the McEvily model can be applied to small physical cracks and can explain various metal fatigue phenomena [13–15]. Due to the superiority of the McEvily model, many scholars used this model to evaluate the fatigue life of materials. Ishihara et al. [14] used the constitutive relationship of the McEvily model to conduct a series of high and low cycle tests during the fatigue life cycle of the titanium alloy to obtain the function relationship between the crack length and the number of loading cycles, and the test results were in good agreement with the predicted results. Luo et al. [15] used the extended McEvily model to predict the fatigue life of surface cracked deep-water structures. The prediction results were compared with the test results, and it was found that the extended McEvily model had better prediction accuracy results than other models. Li et al. [16] compared the newly proposed crack growth models; they found that the improved form of the variable slope of different materials can be explained by the McEvily model, it is capable of predicting fatigue for both short and long fatigue cracks because the McEvily model retains the slope $m$. Nevertheless, the aforementioned research is based on the experiment; the model is challenging to apply to actual bridge engineering because some parameters are impossible to obtain in practice.

To facilitate the practical application of the McEvily fatigue crack growth model. Firstly, an improved McEvily fatigue crack growth model was proposed by simplifying the model parameters with reasonable assumptions and empirical formulas. Then, the model was used to fit the test results of Q345qD steel and compared with the fitting results of the Paris model to verify the effectiveness of the model. Finally, based on the long-term monitoring data of a suspension bridge, the damage value of the fatigue crack in the butt weld of the orthotropic steel deck was calculated by using the improved McEvily model. Compared with the results of the Paris model and nominal stress method, the feasibility of the application of the improved McEvily model in practical engineering was verified. The improved McEvily model proposed in this paper is significant for assessing bridge long-term service performance.

## 2. Improved McEvily Model

### 2.1. Introduction of Paris Model

The study takes the Paris model as a comparison to verify the correctness of the improved McEvily model. The Paris model is given by

$$\frac{da}{dN} = C\Delta K^m, \tag{1}$$

where $da/dN$ is the fatigue growth rate; $\Delta K$ is the range of the stress intensity factor; $C$ and $m$ are material constants, which are the control factors of fatigue crack growth and need to be obtained by fitting the test results.

### 2.2. Improvement of Model Parameters

The McEvilly model mainly explains the problem of fatigue crack growth rate through the effective range of macro crack stress ratio, maximum stress intensity factor, maximum stress intensity factor at the opening level, and stress intensity factor at the threshold level [12]. The McEvily model can be expressed as:

$$\left.\begin{array}{l} \frac{da}{dN} = AM^B \\ M = K_{\max}(1-R) - \left(1-e^{-ka}\right)\left(K_{op\max} - RK_{\max}\right) - \Delta K_{efftth} \\ K_{\max} = \sqrt{\pi r_e\left(\sec\frac{\pi\sigma_{\max}}{2\sigma_V}+1\right)}\left(1+Y(a)\sqrt{\frac{a}{2r_e}}\right)\sigma_{\max} \end{array}\right\}, \quad (2)$$

where $K_{\max}$ is the maximum stress intensity factor; R is the stress ratio ($\sigma_{\max}/\sigma_{\mathrm{mix}}$); $K_{op\max}$ is the maximum stress intensity factor at the opening level for a macroscopic crack; $k$ is a material parameter; $a$ is crack length; $\Delta K_{efftth}$ is the effective range of the stress intensity factor at the threshold level; $r_e$ is an empirical material constant of the inherent flaw length of the order of 1 μm; $\sigma_v$ is the virtual strength of the material; $Y(a)$ is a geometrical factor in calculating the stress intensity factors when under crack length $a$; $A$ and $B$ are material constants, which are the control factors of fatigue crack growth and need to be obtained by fitting the test results.

The fatigue cracks that appear in orthotropic steel decks in the actual engineering bridge are difficult to obtain the relevant parameters through the field test method, so the McEvily model is not ideally used in actual engineering. Therefore, the parameters that are $K_{\max}$, $k$, $K_{op\max}$, and $\Delta K_{efftth}$ in the McEvily model were improved by using reasonable assumptions and empirical formulas to improve.

First, the simplified calculation of $K_{\max}$ is carried out, according to the theory of linear elastic fracture mechanics is obtained

$$\left.\begin{array}{l} \Delta K = K_{\max} - K_{\min} \\ R = \frac{K_{\min}}{K_{\max}} \end{array}\right\}. \quad (3)$$

Thus, $K_{\max}$ can be determined by $\Delta K$ and $R$, namely

$$K_{\max} = \frac{\Delta K}{1-R}. \quad (4)$$

In orthotropic steel bridge decks, the U-rib weld is mainly subjected to the stress along the bridge direction, and the crack of the weld can be regarded as a surface crack subject to the far-field uniform tensile stress [17]. In order to facilitate the analysis of cracks, the cracks assumed to appear in the U-rib butt weld are open cracks. Open cracks are the most common and most likely to cause fracture damage [18]. In order to describe the fatigue crack growth process of the U-rib butt weld, the semi-elliptical surface crack model of the finite thickness plate was employed. Figure 1 shows the semi-elliptical crack surface crack model of the finite thickness plate. According to the linear elastic fracture mechanics, the stress intensity factor of the surface crack in Figure 1 reaches the maximum value at the tip Q [19,20]; its calculation can be expressed as follows:

$$\Delta K = M_1 M_2 \frac{\sigma\sqrt{\pi a}}{E(z)}, \quad (5)$$

where $M_1$ is the free surface coefficient; $M_2$ is the finite plate thickness correction factor; $\sigma$ is the stress range; $E(z)$ is the second type of complete elliptic integrals in calculating the stress intensity factor. The above parameters are given by

$$\left.\begin{array}{c} M_1 = 1 + 0.12(1-a/(2c))^2 \\ M_2 = \left(\frac{2w}{\pi a}\tan\frac{\pi a}{2w}\right)^{\frac{1}{2}} \\ E(z) = \int_0^{\pi/2}\sqrt{1-z^2\sin^2\theta}\,d\theta \\ z^2 = 1-(a/c)^2 \\ \mathrm{W} = \frac{M_1 M_2}{E(z)} \end{array}\right\}, \quad (6)$$

where $a$ is the crack depth; $c$ is the crack width; $w$ is the plate thickness corresponding to the U-rib, and W is the geometric function. During the crack propagation process of Q345qD steel, to simplify the calculation, we supposed $a/c$ = 0.1 is its constant while fatigue crack growth, and then $M_1$ is 1.11, $z$ is 0.995, and $E(z)$ is 1.01. The range of the stress intensity factor could be rewritten as:

$$\Delta K = 1.11 \times \left(\frac{2w}{\pi a} \tan \frac{\pi a}{2w}\right)^{1/2} \frac{\sigma\sqrt{\pi a}}{1.01} \tag{7}$$

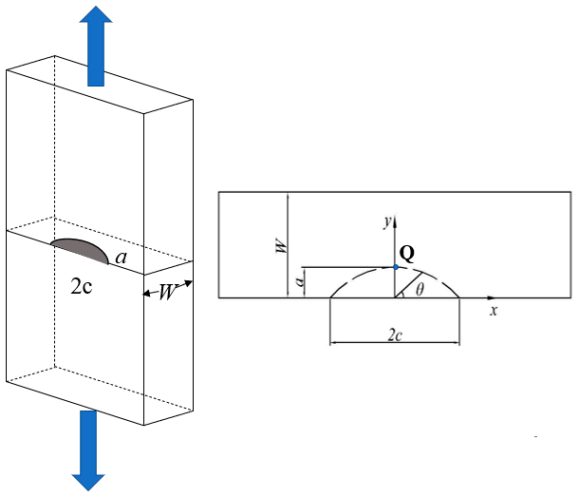



**Figure 1.** The theoretical model of surface cracks.

Then make reasonable assumptions about material parameter $k$. The material parameter $k$ reflects the change of the crack closure effect with the crack length. With the gradual increase in the material parameter $k$, the crack growth rate decrease, and the crack length will also decrease [21]. It is obvious to know that the material parameter $k$ has a certain effect on the crack growth rate. According to the research of Ishihara [22], when calculating surface cracks, the value of $k$ is expressed as a function of crack length $a$, and the expression of the value of $k$ is as follows:

$$k = \begin{cases} \exp(10.6236 - 0.0096228a) & a \le 200\ \mu\text{m} \\ 6000 & a > 200\ \mu\text{m} \end{cases}. \tag{8}$$

Some studies have investigated that the reasonable lower limit of the average initial crack depth of welding details is 0.1 mm, much larger than 200 μm [23–25]. Hence, the paper takes the average value of the initial crack $a_0$ as 0.1 mm, and the material parameter $k$ is set to 6000.

Finally, the parameters of $\Delta K_{effth}$ and $K_{op\max}$ are simplified. Based on the concept of crack closure, through the research of Meggiolaro [26], the $K_{op\max}$ can be defined with

$$\Delta K_{op\max} = K_{\max th} - \Delta K_{effth}, \tag{9}$$

where $K_{\max th}$ is the maximum stress intensity factor at the threshold level.

In order to obtain the empirical formula of $\Delta K_{effth}$, the parameter of $\Delta K_{th}$ is introduced, which is the range of the stress intensity factor range at the threshold. According to the average value of typical specimens used in the fatigue crack growth test, the ratio of $\Delta K_{eff}/\Delta K$ could be determined. The correlation between $\Delta K_{eff}$ and $R$ [27] can be reflected as follows:

$$\Delta K_{eff}/\Delta K = f_{eff} = \begin{cases} 0.52 + 0.42R + 0.06R^2 & R \ge 0 \\ (0.52 - 0.1R)/(1 - R) & -2 \le R < 0' \end{cases} \tag{10}$$

where $\Delta K_{eff}$ is the range of the effective stress intensity factor. Therefore, the ratio of $f_{eff}$ could be obtained according to Equation (10). A quantitative equation of crack growth rate was proposed by Huang et al. [28], which can reflect the crack growth rate under different $R$ by the crack growth rate of $R$ is 0, and $\Delta K_{th}$ can be inferred from $\Delta K_{th0}$:

$$\Delta K_{th}/\Delta K_{th0} = f_{th} = \begin{cases} (1-R)^{0.5} & -5 \le R < 0 \\ (1-R)^{0.3} & 0 \le R < 0.5 \\ (1.05 - 1.4R + 0.6R^2)^{0.3} & 0.5 \le R < 1 \end{cases}, \quad (11)$$

where $\Delta K_{th0}$ is the threshold stress intensity factor range when $R$ is 0.

According to the Equations (9)–(11), $\Delta K_{effth}$ and $K_{op\max}$ could be rewritten as:

$$\Delta K_{effth} = f_{eff} f_{th} \Delta K_{th0}, \quad (12)$$

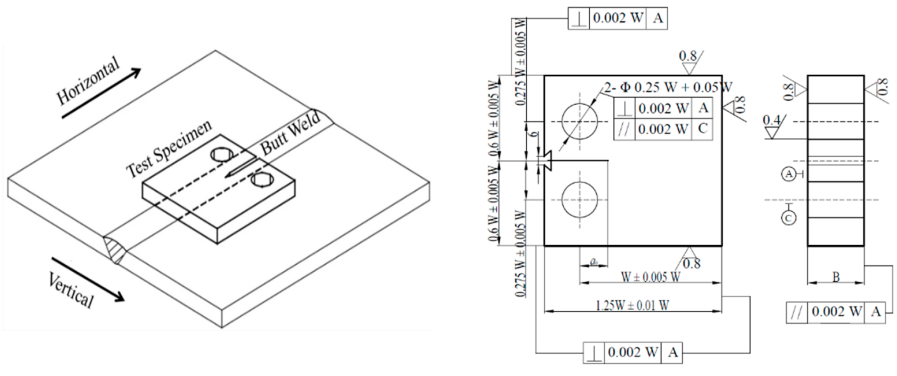
$$\Delta K_{op\max} = K_{\max th} - \Delta K_{effth} = [1/(1-R) - f_{eff}] f_{th} \Delta K_{th0}, \quad (13)$$

when the above parameters are determined through assumptions and empirical formulas, the McEvily model can be modified as follows:

$$\left.\begin{array}{l} \frac{da}{dN} = AM^B \\ M = [1 + \frac{R}{1-R}(1 - e^{-ka})]\Delta K - \frac{1-e^{-ka}}{1-R} f_{th} \Delta K_{th0} - e^{-ka} f_{eff} f_{th} \Delta K_{th0} \\ \Delta K = 1.11 \times (\frac{2w}{\pi a} \tan \frac{\pi a}{2w})^{1/2} \frac{\Delta \sigma \sqrt{\pi a}}{1.01} \end{array}\right\}. \quad (14)$$

### 2.3. The Effectiveness of Improved McEvily Model

In order to prove the effectiveness of the improved McEvily model, the typical steel structure fatigue crack (fatigue crack of butt weld of orthotropic steel deck) was selected for analysis in this study, and the experimental research data of Q345qD steel were cited. Liang et al. [29] conducted experiments on the fatigue crack growth rate of metallic materials. The different thickness specimens and different stress ratios were used for the experimental research, and the fully automated crack length measurement software was used for collecting data. By means of data processing, the fatigue crack growth rate curves of 6.1 mm, 10.0 mm, and 23.5 mm thickness weld specimens under different stress ratios (R = 0.1, 0.2, 0.5) were obtained. The test specimens were made according to the mechanical standard of GB/T 714-2008 specification [30], in which the schematic diagram of the test specimens is shown in Figure 2a, and the dimensions of the test specimens are shown in Figure 2b. The basic mechanical properties of Q345qD butt welds were measured by uniaxial tensile test, and the average mechanical properties of Q345qD butt welds: $f_y$ is 534 MPa, $f_u$ is 596 MPa, $E$ is 2.51 × $10^5$ MPa.




(**a**) (**b**)

**Figure 2.** Geometry of test specimens, (**a**) The schematic diagram of test specimens, (**b**) The dimensions of the test specimens.

The improved model was validated numerous times in this paper using the experimental data. Due to the presence of the weld, the test results for the same specimen subjected to the same stress ratio remain somewhat dissimilar. In this study, the above dissimilar is mainly manifested in the change of the material constants (as shown in Table 1 and Figures 3–5). As a result, the establishment of different Paris models is essential to exactly estimate the fatigue crack growth rate for the same specimens with different material constants. Compared to the Paris model, the improved McEvily model has extremely robust against the effects of welds. Just one improved McEvily model for the same specimen is required. The improved McEvily model, based on the same specimen, is only related to stress ratios, which significantly improves computing efficiency and engineering application.

**Table 1.** Comparison of material constants under the two models [29].

| The Thickness of Specimen | Stress Ratio | Material Constants of the Paris Model | | Material Constants of the Improved McEvily Model | |
|---|---|---|---|---|---|
| | | $\overline{m}$ | $\overline{\lg C}$ | $\overline{B}$ | $\overline{\lg A}$ |
| 6.1 mm | 0.1 | 2.63 | −10.78 | 2.53 | −10.65 |
| | 0.2 | 2.51 | −10.39 | | |
| | 0.5 | 2.69 | −10.56 | | |
| 10.0 mm | 0.1 | 2.68 | −10.88 | 2.58 | −10.79 |
| | 0.2 | 3.04 | −11.41 | | |
| | 0.5 | 2.84 | −11.07 | | |
| 23.5 mm | 0.1 | 2.40 | −10.61 | 2.61 | −11.11 |
| | 0.2 | 3.32 | −12.23 | | |
| | 0.5 | 3.02 | −11.45 | | |

The validation procedure is demonstrated here by utilizing a specimen set consisting of 6.1 mm thick nine specimens (as shown in Table 1 and Figure 3). Firstly, the specimen set was divided into three working conditions with stress ratios of 0.1, 0.2, and 0.5, and the average value of material constants was computed for each set of working conditions using experimental data (as shown in Table 1). Second, three Paris models with different material constants were established based on experimental data to predict the fatigue crack growth rate at various stress ratios, respectively. Then, an improved McEvily model was established based on the test data of three specimens with a stress ratio equal to 0.5. The experimental data of the sample set with a stress ratio of 0.5 is the most concentrated, and the accuracy of the established improved McEvily model can be enhanced (as shown in Figure 3c). Finally, the established McEvily model was applied to specimen sets with stress ratios of 0.2 and 0.3. The accuracy of the fitting results was proven by comparing with the fatigue crack growth rate curves of Paris models (as shown in Figure 3).

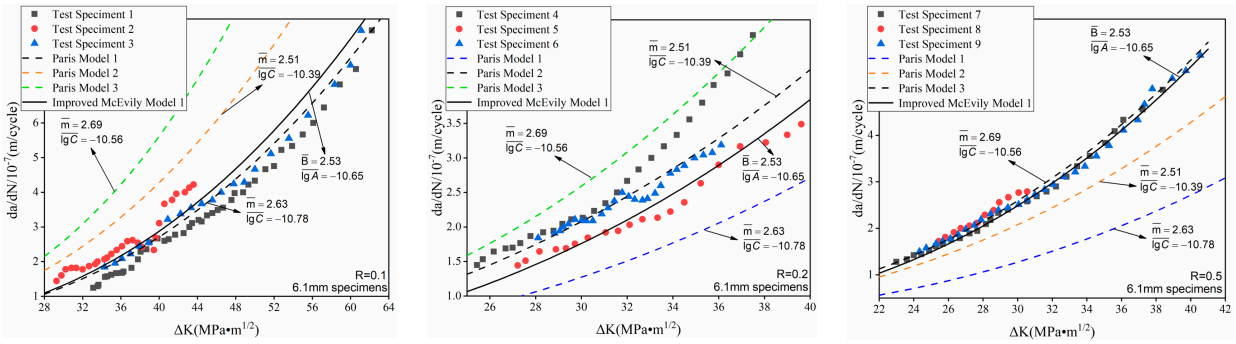



**Figure 3.** Comparison of fatigue crack growth models of 6.1 mm specimens. (**a**) R is 0.1; (**b**) R is 0.2; (**c**) R is 0.5.

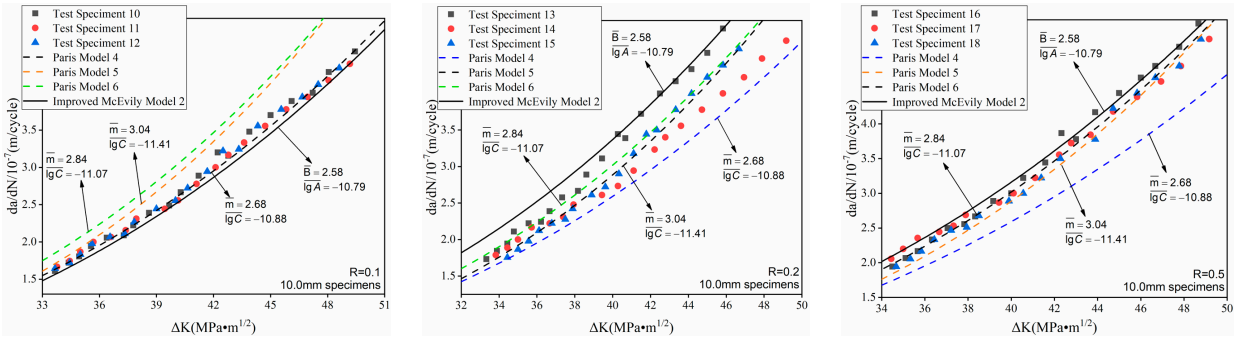



**Figure 4.** Comparison of fatigue crack growth models of 10.0 mm specimens. (**a**) R is 0.1; (**b**) R is 0.2; (**c**) R is 0.5.

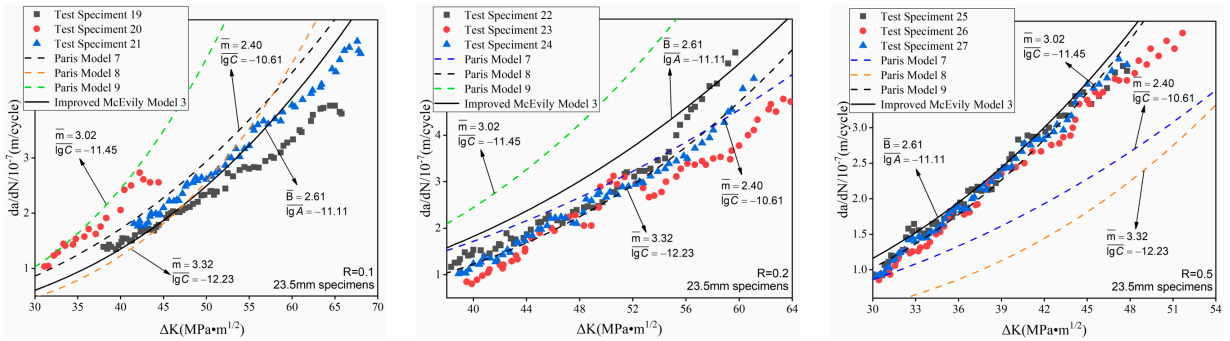



**Figure 5.** Comparison of fatigue crack growth models of 23.5 mm specimens. (**a**) R is 0.1; (**b**) R is 0.2; (**c**) R is 0.5.

Fatigue fracture growth rate curves of improved McEvily models are highly similar to results obtained from experiments and the Paris models, as shown in Figures 3–5. It proves that for the same sample thickness, the improved McEvily model requires only a set of stress ratio experimental to determine the material constant, which overcomes the influence of the weld. Further demonstrates that the improved McEvily model has good robustness and applicability.

In order to be able to apply the improved McEvily model to the practical engineering, according to the fitting results of the material constants of the above Q345qD steel, the material constants lg$A$, and $B$ used in this paper are −10.65 and 2.53, respectively. The improved McEvily model is as follows:

$$\frac{da}{dN} = 2.2387 \times 10^{-11} M^{2.53}. \tag{15}$$

## 3. The Verification of Engineering Feasibility

In order to verify the feasibility of the improved McEvily model in practical engineering, the fatigue crack of the Q345qD steel butt weld of a suspension bridge was analyzed. Based on the long-term strain monitoring data, the improved McEvily model, Paris model, and nominal stress method were used to calculate the fatigue damage value of the monitoring location.

### *3.1. The Processing of Monitoring Data*

The study selected a strain monitoring point SG15 on the suspension bridge to analyze the strain gauge SG15 is located in the middle of the bridge span, which is subject to vehicle load all year round and is prone to fatigue cracks. The installation location of the strain

gauge is shown in Figure 6. One-day data of SG15 were used to analyze the characteristics of original strain monitoring data. Figure 7a shows the strain history for 864,000 data points recorded on one day in 2015. The generation of the strain−time curve contains three factors: (1) temperature-induced strain change: temperature mainly affects the overall trend of the average strain and the induced strain changes with a small amplitude. (2) random ambient excitations (including noise): plenty of signals which are low in amplitudes and show a continuous distribution. (3) random vehicle load: the strain amplitude caused by the vehicle load changes greatly, and there are obvious troughs and peaks, which are the main reasons for the fatigue crack growth in the structural details.

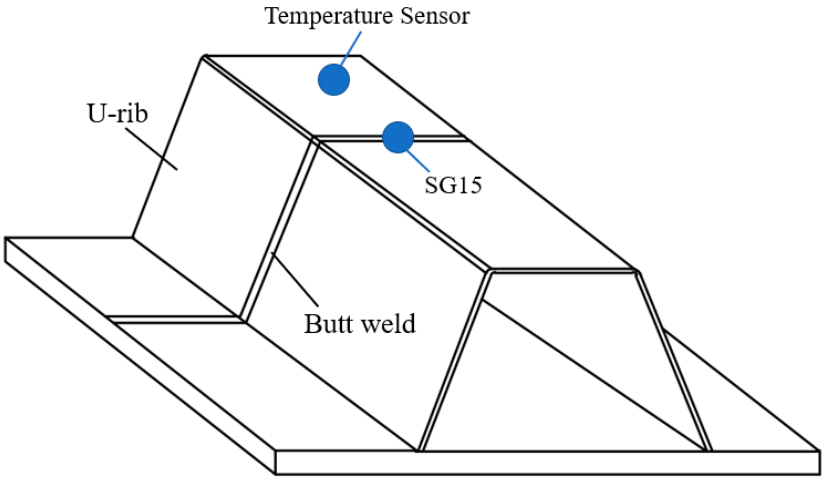



**Figure 6.** Stress gauge SG15 and temperature sensor location.

Firstly, the influence curve of temperature on the strain signal was separated. The installation location of the temperature sensor is shown in Figure 6. Using wavelet transform [31], the original signal was decomposed by multi-scale wave decomposition and reconstructed in the low-frequency band. Then, the mean strain caused by the temperature was obtained, as shown in Figure 7b. Figure 7b shows the strain−time curve affected by temperature and temperature−time curve in the steel box girder. It can be seen that the strain−time curve lags behind the temperature−time curve, but their periodic variation trends are generally the same. Temperature mainly affects the trend of the overall strain and has little effect on the variation of the strain amplitude, which the amplitude variation time is relatively long.

Secondly, the effects of random excitations and measurement noise on strain were separated. Wavelet transform was performed on the original signal, and thresholds were selected for signal processing according to the features at different scales. After the signals were extracted, the multi-scale random environmental excitations influence signals were reconstructed to obtain their strain−time curve, as displayed in Figure 7c. Figure 7d shows the strain–time curve caused by the vehicle load after removing the effect of other factors. This study mainly used the fracture mechanics method and Nominal stress method to calculate the damage value of fatigue crack and analyzed the strain−time curve under the influence of vehicle load; R has a correlation with vehicle load, here R = 0 (as shown in Figure 7d).

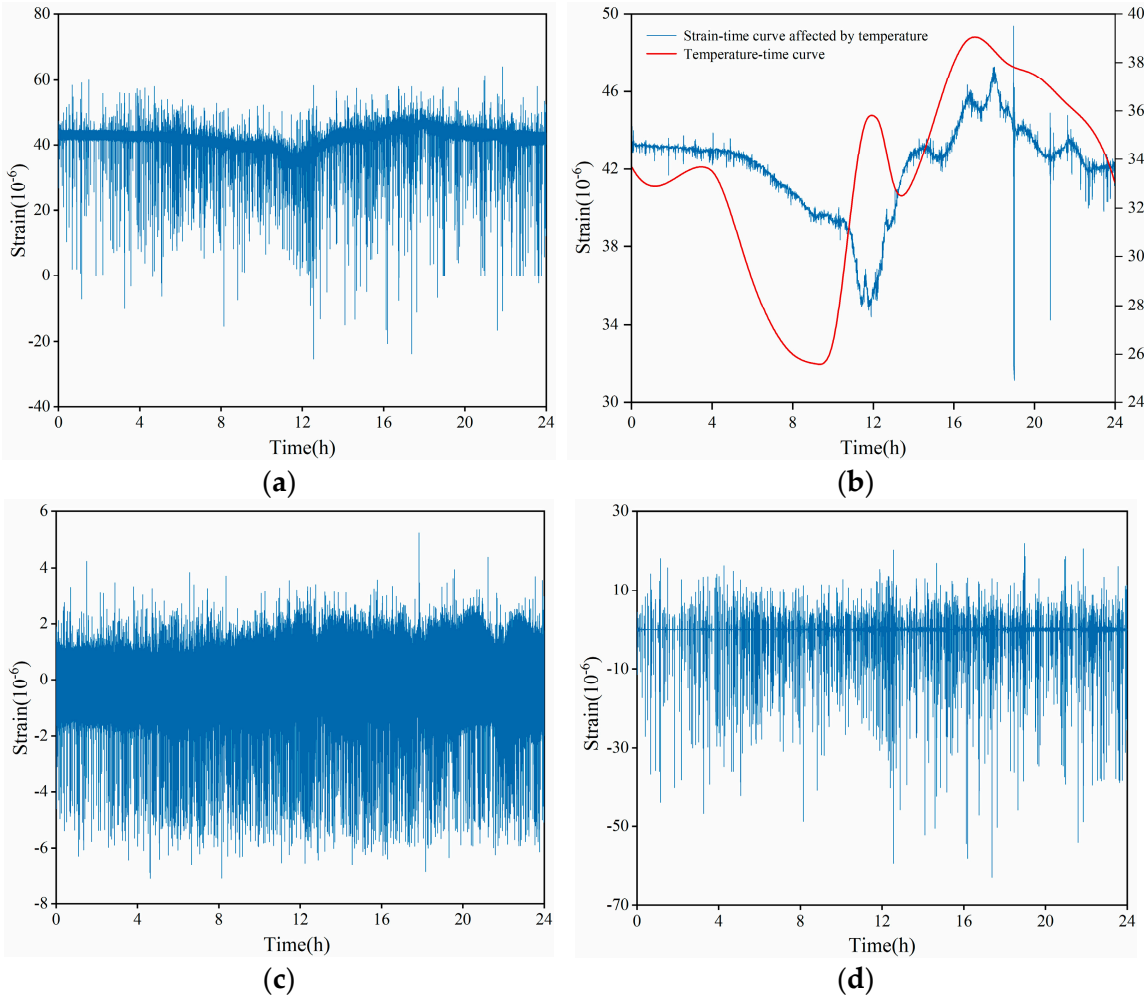



**Figure 7.** Signal of gauge SG15. (**a**) Original strain–time curve; (**b**) Strain−time curve affected by temperature; (**c**) Strain–time curve caused by random ambient excitations; (**d**) Strain–time curve caused by vehicle loads.

### *3.2. Calculation of Fatigue Crack Growth*

The annual fatigue crack depth is the key index to calculate the fatigue crack damage value by the fracture mechanics method. Firstly, the number of load cycles needs to be analyzed according to the monitoring data, the strain−time curve in Figure 7d can be transformed into the stress−time curve by multiplying the elastic modulus, and the stress range was extracted from the stress–time curve using rain−flow counting method [32], the stress range $\sigma_i$ was from 0 to 35 MPa, as shown in Figure 8. According to Miner's damage accumulation theory [33], the daily effective stress range $\sigma_e$ under the variable amplitude load is expressed as

$$\sigma_e = \left(\sum \frac{n_i}{N_a}\sigma_i^m\right)^{1/m}, \tag{16}$$

where $n_i$ is the number of cycles of the stress range $\sigma_i$; $N_a$ is the number of cycles of all the stress ranges; $m$ is related to material properties.

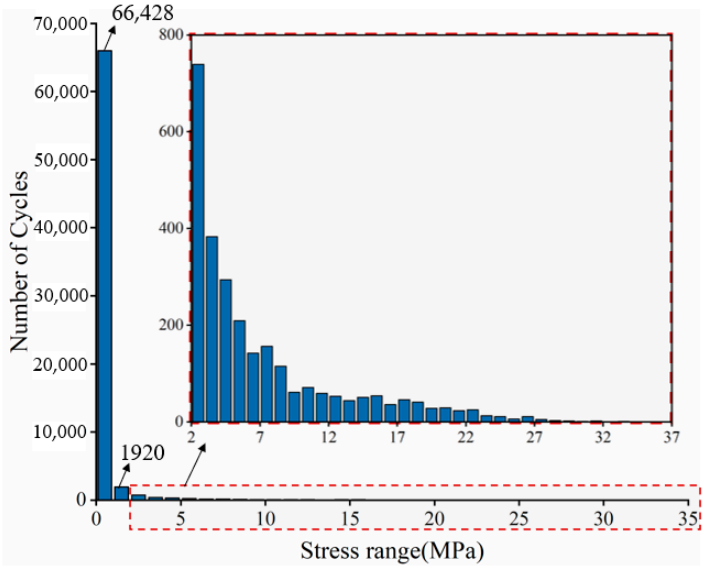



**Figure 8.** Stress range cycle number of gauge SG15.

Due to the effective daily stress range, $\sigma_e$ is a random variable, the mean value of the effective daily stress range is represented as

$$E(\sigma) = \int_0^{+\infty} \sigma_e f(\sigma) d\sigma_e, \tag{17}$$

where $f(\sigma)$ is the probability density of the daily effective stress range.

Secondly, the cumulative damage induced by repetitive vehicle load actions is the primary source of steel bridge fatigue damage. Thus, the growth of traffic flow needs to be considered in calculating the fatigue crack depth. The subjects of this study were a significant amount of field data acquired from the suspension bridge's health monitoring system between 2010 and 2018. Based on the known traffic flow from 2010 to 2015 years, the gray theory [34] is used to predict the traffic flow from 2016 to 2040 years. The prediction model of the annual traffic flow of the suspension bridge is:

$$\left.\begin{array}{c} \hat{x}^{(1)}(t+1) = 4223.976143 \times e^{3.018} - 3909.976143 \\ \hat{x}^{(0)}(t+1) = \hat{x}^{(1)}(t+1) - \hat{x}^{(1)}(t) \end{array}\right\}, \tag{18}$$

where $\hat{x}^{(1)}(t)$ is the cumulative annual traffic flow from 2010 to $t$. $\hat{x}^{(0)}(t+1)$ is the annual traffic flow in year $(t+1)$.

Figure 9 shows the traffic flow from 2016 to 2040 predicted by the gray theory. The maximum error of the comparison between the actual traffic flow and the predicted traffic flow in 2016−2018 is not more than 5%, indicating that the accuracy of the predicted traffic flow can be verified, which can be seen in Figure 9. The data curve fitting of the predicted traffic flow shows that the annual traffic flow increases exponentially at a 10.56% growth rate. Then, the number of stress cycles of vehicle load within one year $X(t)$ is

$$X(t) = 365 \times X_d \times (1+z)^t, \tag{19}$$

where $X_d$ is the mean of the number of daily stress cycles corresponding to the mean of the daily effective stress ranges $E(\sigma)$; $z$ is the annual traffic growth rate.

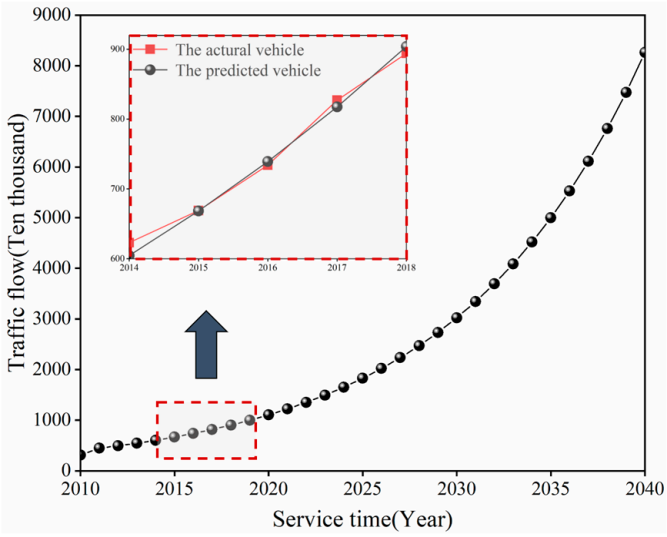



**Figure 9.** Traffic flow predicted by Grey Theory.

Finally, based on the stress range cycle number histogram and the predicted annual traffic flow, the study used the Markov chain [35] to analyze and obtain the annual fatigue crack depth. Figure 10 showed crack depth increment predicted by the improved McEvily model and the Paris model, in which $C$ and $m$ used in Paris model are $7.158 \times 10^{-11}$ and 3, respectively, according to the Eurocode 3 [36]. From Figure 10, it can be seen that the crack depth increases exponentially with the increase in annual traffic flow. The crack growth predicted by the two models increases slowly in the initial stage and rapidly in the later stage, which is consistent with the phenomenon observed in practical engineering. The crack depth increment predicted by the improved McEvily model is not much different from that predicted by the Paris model in the initial stage. With the growth of time, the gap between the crack growth predicted by the two models gradually widens. The final crack depth increment predicted by the improved McEvily model is 32.4% larger than that predicted by the Paris model, and the prediction result is more conservative. The study analyzed the small vehicle load without considering the negative factors such as heavy or super heavy vehicle load and corrosion, so the predicted crack depth developed slowly.

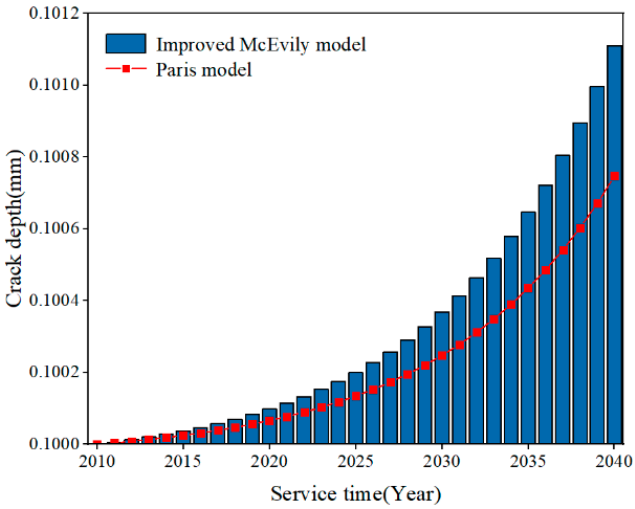



**Figure 10.** Crack depth growth curve.

### *3.3. Comparison of Crack Fatigue Damage*

The nominal stress method is one of the most commonly used methods to evaluate fatigue cracks, and the calculated results of this method are relatively conservative. In

order to compare the calculation results of the improved McEvily model with the nominal stress method, the fatigue crack damage value index was used in this section. The nominal stress method based on Eurocode 3 was introduced, and the $S-N$ curve of Eurocode 3 is shown in Figure 11.

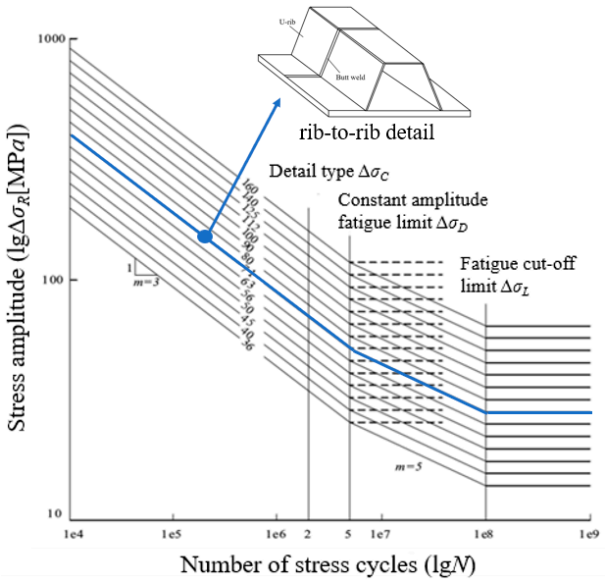



**Figure 11.** $S-N$ curve of Eurocode 3.

For the nominal stress method, Eurocode 3 provides the fatigue strength curves based on:

$$\Delta\sigma_R^3 N_R = \Delta\sigma_C^3 \cdot 2 \times 10^6 = K_C \left(N \le 5 \times 10^6\right), \tag{20}$$

$$\Delta\sigma_R^5 N_R = \Delta\sigma_D^5 \cdot 5 \times 10^6 = K_D \left(5 \times 10^6 \le N \le 10^8\right), \tag{21}$$

where $\Delta\sigma_R$ is the stress range; $N_R$ is the corresponding life expressed as the number of cycles related to $\Delta\sigma_R$; $\Delta\sigma_C$ is the fatigue strength when fatigue life is $2 \times 10^6$ cycles. $\Delta\sigma_D$ is the fatigue strength when fatigue life is $5 \times 10^6$ cycles; $K_C$ and $K_D$ are fatigue strength coefficients. According to Eurocode 3, $K_C$ and $K_D$ of the rib-to-rib welded details are $7.16 \times 10^{11}$ and $1.90 \times 10^{15}$, respectively.

Therefore, the fatigue damage value of the stress range histogram can be defined as

$$D = \sum_{S_i \ge \Delta\sigma_D} \frac{n_i S_i^3}{K_C} + \sum_{S_j \le \Delta\sigma_D} \frac{n_j S_j^5}{K_D}, \tag{22}$$

where $n_i$ is the number of stress range $S_i$, which is bigger than $\Delta\sigma_D$; and $n_j$ is the number of stress range $S_j$.

In order to observe the fatigue damage value caused by each stress range, the fatigue damage histogram of strain gauge SG15 can be obtained through Figure 8 and Equation (22); the results are shown in Figure 12. Based on the actual annual traffic growth rate of 10.56%, the paper forecasted the fatigue damage value of SG15 from 2010 to 2040, and the annual fatigue damage value $D_{total}$ is

$$D_{total} = \frac{x_t {\sigma_e}^5}{K_D} = 365 \times X_d \times (1+z)^t \frac{\sigma_e^5}{K_D}. \tag{23}$$

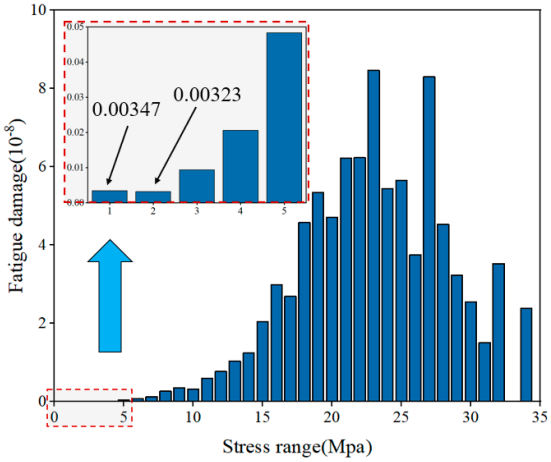



**Figure 12.** Fatigue damage histogram of gauge SG15.

The prediction results of the nominal stress method are shown in Figure 13.

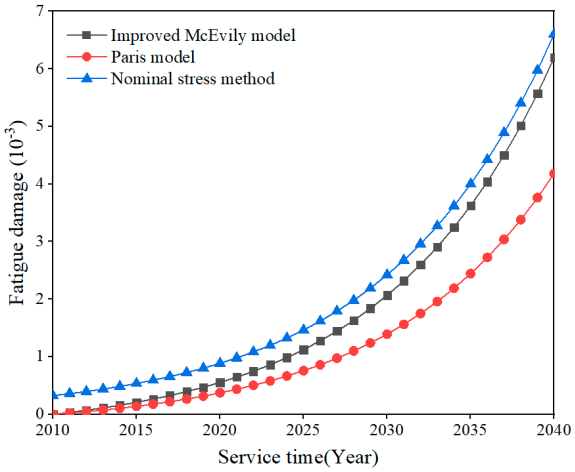



**Figure 13.** Fatigue damage prediction results.

Based on the theory of linear elastic fracture mechanics, the prediction of fatigue crack depth from 2010 to 2040 can be converted into annual fatigue damage according to Equations (24) and (25). The expression of annual fatigue damage value is

$$n_i = \int_{a_i}^{a_c} \frac{da}{2.2387(M(a))^{2.53}}, \quad i = 2010, 2011, \ldots, 2040, \tag{24}$$

$$D_{total} = 1 - \frac{n_i}{n_{2010}}. \tag{25}$$

The annual fatigue damage value of the improved McEvily model and Paris model in 2010–2040 is shown in Figure 13, and the initial fatigue damage value is 0. From Figure 13, it can be seen that the fatigue damage value calculated by the improved McEvliy model is similar to the nominal stress method. Since the improved McEvliy model considers more engineering factors, the growth rate is greater than that calculated by the nominal stress method. The Paris model is significantly less than the nominal stress method and the improved McEvily model in the calculated results, which cannot accurately evaluate the fatigue crack life. Because the Paris model has limited in predicting the fatigue life of small cracks, resulting in smaller calculated results. It shows that the accuracy of the improved McEvily model in the calculated results is greater than that of the Paris model and can be well adapted to practical engineering. The improved McEvily model can preliminarily

evaluate the fatigue crack life, providing convenience for bridge managers and ensuring the safety of orthotropic steel bridge decks.

## 4. Conclusions

In the current field of fatigue life prediction of steel structures, the classical Paris model cannot reflect the influence of different stress ratios and cannot be applied to the growth of small cracks. The original McEvily model is difficult to apply in practical engineering due to the complexity of its parameters. Based on the above limitations, the paper proposes an improved McEvily model. Firstly, the calculation methods of the four parameters $K_{\max}$, $k$, $K_{op\max}$, and $\Delta K_{effth}$ of the McEvily model in the existing references were simplified, and its application range was extended from experimental conditions to practical engineering. Then, based on the Q345qD steel test data, the fitting results of the Paris model were compared to verify the correctness of the improved McEvily model. Furthermore, the improved McEvily model solves the weakness of the Paris model, and it has robust to the influence of welds. The improved McEvily model has broader applicability in real engineering than the Paris model. Finally, the improved McEvily model was used in practical engineering to verify its effectiveness. Based on the long-term monitoring data, the fatigue damage index was used to evaluate the fatigue crack of the U-rib. The calculation results of the improved McEvily model were compared with the Pairs model and the nominal stress method, which reflects the accuracy of the model in evaluating the fatigue crack life of steel structures. Overall, the improved McEvily model provides a more accurate theory for calculating the fatigue life of steel structures and has a certain reference value for bridge engineers to evaluate the fatigue life of steel structures. However, the improved McEvily model can only be used in the case of open cracks, and the fatigue prediction of other forms of steel structure cracks deserves further discussion.

**Author Contributions:** Conceptualization, Z.Y. and J.W.; methodology, Z.Y. and K.M.; formal analysis, Z.Y.; software, Z.Y. and C.Z.; writing—original draft preparation, Z.Y.; writing—review and editing, Z.Y. and C.J. All authors have read and agreed to the published version of the manuscript.

**Funding:** This research received no external funding.

**Institutional Review Board Statement:** Not applicable.

**Informed Consent Statement:** Informed consent was obtained from all subjects involved in the study.

**Data Availability Statement:** All data, models, and code generated or used during the study appear in the submitted article.

**Conflicts of Interest:** The authors declare no conflict of interest.

## References

1. Fisher, J.W.; Barsom, J.M. Evaluation of cracking in the rib-to-deck welds of the bronx–whitestone bridge. *J. Bridge Eng.* **2016**, *21*, 04015065. [CrossRef]
2. Kainuma, S.; Yang, M.; Jeong, Y.S.; Inokuchi, S.; Kawabata, A.; Uchida, D. Experiment on fatigue behavior of rib-to-deck weld root in orthotropic steel decks. *J. Constr. Steel Res.* **2016**, *119*, 113–122. [CrossRef]
3. Heng, J.L.; Zheng, K.F.; Gou, C.; Zhang, Y.; Bao, Y. Fatigue performance of rib-to-deck joints in orthotropic steel decks with thickened edge U-ribs. *J. Bridge Eng.* **2017**, *22*, 0417059. [CrossRef]
4. Imam, B.M.; Chryssanthopoulos, M.K. A Review of Metallic Bridge Failure Statistics. In *Bridge Maintenance, Safety and Management, Proceedings of the Fifth International IABMAS Conference, Philadelphia, PA, USA, 11–15 July 2010*; CRC Press: Boca Raton, FL, USA, 2010.
5. Macdougall, C.; Green, M.F.; Shillinglaw, S. Fatigue damage of steel bridges due to dynamic vehicle loads. *J. Bridge Eng.* **2006**, *11*, 320–328. [CrossRef]
6. Xiao, Z.G.; Yamada, K.; Ya, S.; Zhao, X.L. Stress analyses and fatigue evaluation of rib-to-deck joints in steel orthotropic decks. *Int. J. Fatigue* **2008**, *30*, 1387–1397. [CrossRef]
7. Dorin, R.; Aleksandar, S.; Simon, S.; Wei, L. Engineering critical assessment of steel shell structure elements welded joints under high cycle fatigue. *Eng. Fail. Anal.* **2020**, *114*, 104578.
8. Ding, Z.; Wang, X.; Gao, Z.; Bao, S. An experimental investigation and prediction of fatigue crack growth under overload/underload in Q345R steel. *Int. J. Fatigue* **2017**, *98*, 155–166. [CrossRef]

9. Xiang, Z.; Gaenser, H.P.; Pippan, R. The effect of single overloads in tension and compression on the fatigue crack propagation behaviour of short cracks. *Int. J. Fatigue* **2016**, *89*, 77–86.
10. Paris, P.C.; Erdogan, F. A critical analysis of crack propagation laws. *J. Basic Eng.* **1963**, *85*, 528–533. [CrossRef]
11. Forman, R.G.; Kearney, V.E.; Engle, R.M. Numerical analysis of crack propagation in cyclic-loaded structures. *J. Basic Eng.* **1967**, *49*, 459–464. [CrossRef]
12. Mcevily, A.J.; Ishihara, S.; Endo, M. An analysis of multiple two-step fatigue loading. *Int. J. Fatigue* **2005**, *27*, 862–866. [CrossRef]
13. Endo, M.; Mcevily, A.J. Prediction of the behavior of small fatigue cracks. *Mater. Sci. Eng. A* **2007**, *468*, 51–58. [CrossRef]
14. Ishihara, S.; McEvily, A.J. Analysis of short fatigue crack growth in cast aluminum alloys. *Int. J. Fatigue* **2002**, *24*, 1169–1174. [CrossRef]
15. Luo, G.E.; Cui, W.C. Fatigue crack propagation of the surface cracked deepwater structures based on extended mcevily model. *J. Ship Mech.* **2013**, *17*, 645–655.
16. Li, Y.X.; Cui, W.C.; Zhang, W.M. A modified constitutive relation for fatigue crack growth. *J. Ship Mech.* **2006**, *10*, 54–61. (In Chinese)
17. Fett, T. Estimation of stress intensity factors for semi-elliptical surface cracks. *Eng. Fract. Mech.* **2000**, *66*, 349–356. [CrossRef]
18. Nagy, W.; Schotte, K.; Bogaert, P.V.; Backer, H.D. Fatigue strenght application of fracture mechanics to orthotropic steel decks. *Adv. Struct. Eng.* **2016**, *19*, 1696–1709. [CrossRef]
19. Sih, G.C. *Handbook of Stress-Intensity Factors for Researchers and Engineers*; Bethlehem, P.A., Ed.; Institute of Fracture and Solid Mechanics: Bethlehem, PA, USA, 1973.
20. Guo, T.; Chen, Y.W. Fatigue reliability analysis of steel bridge details based on field-monitored data and linear elastic fracture mechanics. *Struct. Infrastruct. Eng.* **2013**, *9*, 496–505. [CrossRef]
21. Mcevily, A.J.; Ishihara, S. On the dependence of the rate of fatigue crack growth on the $\sigma^n{}_a$ (2a) parameter. *Int. J. Fatigue* **2001**, *23*, 115–120. [CrossRef]
22. Ishihara, S.; Mcevily, A.J. A coaxing effect in the small fatigue crack growth regime. *Scr. Mater.* **1999**, *42*, 617–622. [CrossRef]
23. Xiao, Z.G.; Yamada, K.; Inoue, J.; Yamaguchi, K. Fatigue cracks in longitudinal ribs of steel orthotropic deck. *Int. J. Fatigue* **2005**, *28*, 409–416. [CrossRef]
24. Righiniotis, T.D.; Chryssanthopoulos, M.K. Probabilistic fatigue analysis under constant amplitude loading. *J. Constr. Steel Res.* **2003**, *59*, 867–886. [CrossRef]
25. Uwe, Z.; Mauro, M.; Michael, V. Applying fracture mechanics to fatigue strength determination—Some basic considerations. *Int. J. Fatigue* **2019**, *126*, 188–201.
26. Meggiolaro, M.A.; Castro, J.T.P.D. On the dominant role of crack closure on fatigue crack growth modeling. *Int. J. Fatigue* **2003**, *25*, 843–854. [CrossRef]
27. Newman, J.; Crews, J.; Bigelow, C.A.; Dawicke, D.S. Variations of a global constraint factor in cracked bodies under tension and bending loads. *ASTM Spec. Tech. Publ.* **1995**, *1224*, 21–42.
28. Huang, X.; Torgeir, M.; Cui, W. An engineering model of fatigue crack growth under variable amplitude loading. *Int. J. Fatigue* **2008**, *30*, 2–10. [CrossRef]
29. Liang, Z.; Gang, S.; Wang, Y. Experimental investigation on fatigue crack behavior of bridge steel Q345qD base metal and butt weld. *Mater. Des.* **2015**, *66*, 196–208.
30. GB/T 714-2008. Structural Steel for Bridge. Standards Press of China: Beijing, China, 2008. (In Chinese)
31. Taha, M.R.; Noureldin, A.; Lucero, J.L.; Baca, T.J. Wavelet transform for structural health monitoring: A compendium of uses and features. *Struct. Health Monit.* **2006**, *5*, 267–295. [CrossRef]
32. Deng, Y.; Liu, Y.; Feng, D.M.; Li, A.Q. Investigation of fatigue performance of welded details in long-span steel bridges using long-term monitoring strain data. *Struct. Control Health Monit.* **2015**, *22*, 1343–1358. [CrossRef]
33. Siwowski, T.; Kulpa, M.; Janas, L. Remaining fatigue life prediction of welded details in an orthotropic steel bridge deck. *J. Bridge Eng.* **2019**, *2*, 0519013.1–05019013.14. [CrossRef]
34. Yang, Y.C. An urban rail transit hazard evaluation methodology based on grey system theory. *Procedia Soc. Behav. Sci.* **2012**, *43*, 764–772.
35. Gansted, L.; Brincker, R.; Hansen, L.P. Fracture mechanical Markov chain crack growth model. *Eng. Fract. Mech.* **1991**, *38*, 475–489. [CrossRef]
36. *BS EN 1993-1-9:2005*; Eurocode 3: Design of Steel Structures-Part 1–9: Fatigue. European Committee for Standardization: Cardiff, UK, 2005.